International Journal of Thermal Sciences 48 (2009) 1007–1016

Contents lists available at ScienceDirect

International Journal of Thermal Sciences

www.elsevier.com/locate/ijts

Performance evaluation of solar air heater having expanded metal mesh as artificial roughness on absorber plate

M.K. Gupta *, S.C. Kaushik

Centre for Energy Studies, Indian Institute of Technology, Delhi 110016, India

ARTICLE INFO

Article history:
Received 29 March 2008
Received in revised form 22 August 2008
Accepted 25 August 2008
Available online 23 September 2008

Keywords:
Solar air heater
Expanded metal mesh
Roughness geometry parameter
Energy augmentation ratio
Effective energy augmentation ratio
Exergy augmentation ratio
Reynolds number

ABSTRACT

A parametric study of artificial roughness geometry of expanded metal mesh type in the absorber plate of solar air heater duct has been carried out and compared with smooth duct. The performance evaluation in terms of energy augmentation ratio (*EAR*), effective energy augmentation ratio (*EEAR*) and exergy augmentation ratio (*EXAR*) has been carried out for various values of Reynolds number (*Re*) and roughness parameters of expanded metal mesh roughness geometry in the absorber plate of solar air heater duct. It is found that the augmentation ratios decrease at faster rate with *Re* in the order of *EAR*, *EEAR* and *EXAR*. It is also found that augmentation ratios increase with increase in duct depth and intensity of solar radiation. The artificially roughened solar air heater duct performs better as per *EAR* or heat energy gain criteria for any values of *Re* and roughness parameters of expanded metal mesh. The *EAR* is high for the parameters of expanded metal mesh type roughness geometry which create more turbulence, however the pump work required for flow of air will also increase. The *EXAR* is a more suitable criterion to incorporate the quality of heat collected and pump work required. The *EXAR* is more for higher duct depth and low *Re* range. Based on *EXAR* the suitable design parameters of expanded metal mesh roughness geometry are determined.

1. Introduction

The heat transfer between the absorber surface (heat transfer surface) of solar air heater and flowing air can be improved by increasing heat transfer coefficient using the turbulence promoters in the form of artificial roughness on absorber surface [1]. Varun et al. [1] presented a review of various types of roughness geometry used in solar air heaters. Many investigators analyzed various roughness geometry [1–4] and attempted to develop accurate predictions of the heat-transfer coefficient and friction factor of a given roughness geometry, and to define a roughness geometry which gives the best heat-transfer performance for a given flow friction. Saini and Saini [5] carried out experimental investigation for fully developed turbulent flow in a rectangular duct having expanded metal mesh as artificial roughness. They developed correlations for Nusselt number and friction factor in terms of geometry of expanded metal mesh.

The artificial roughness that results in the desirable increase in the heat-transfer also results in an undesirable increase in the pressure drop due to the increased friction. Several researchers carried out the thermo-hydraulic performance evaluation on the basis of effective efficiency [4]. To balance the quality of useful heat energy and friction losses, second law of thermodynamics based exergy is a suitable quantity for the optimization of roughness geometry parameters of solar air heaters. Exergy is maximum work potential which can be obtained from a form of energy [6,7]. Recently, the concept of exergy has received great attention from scientists, researchers and engineers, and exergy concept has been applied to various utility sectors and thermal processes. The popularity of exergy analysis method has grown consequently and is still growing [6,8–10]. The exergy based performance evaluation of solar air heater duct having artificial roughness on absorber plate has attracted less attention of researchers so far. Ucar and Inalli [11] carried out the experimental exergy based performance evaluation of solar air heaters having passive heat transfer augmentation techniques. They tested solar air heaters with staggered absorber plates, and staggered fins attached on absorber and bottom plates. Esen [12] experimentally evaluated the energy and exergy efficiency of four types of double-flow (flow above and below the absorber plate) flat plate solar air heater with obstacles and without obstacles on absorber plate. Layek et al. [13] numerically calculated the augmentation entropy generation number [7] in the duct of solar air heater having repeated transverse integral chamfered rib–groove roughness on one broad heated wall. Though the integral chamfered rib–groove roughness geometry creates more turbulence, but it requires the machining of the relatively thick absorber plate.

* Corresponding author. Tel.: +91 11 26591253; fax: +91 11 26862037.
E-mail addresses: mk_gupta70@rediffmail.com (M.K. Gupta), kaushik@ces.iitd.ac.in (S.C. Kaushik).

1290-0729/$ – see front matter
doi:10.1016/j.ijthermalsci.2008.08.011

Nomenclature

A_c	collector area	m^2
C_f	conversion factor	
c_p	specific heat	J/kg K
d_e	equivalent hydraulic diameter of collector duct	m
e	rib height	m
EAR	energy augmentation ratio	
$EEAR$	effective energy augmentation ratio	
Ex	exergy	W
$EXAR$	exergy augmentation ratio	
$Ex_{c,S}$	exergy of solar radiation incident on glass cover	W
Ex_u	exergy output rate ignoring pressure drop	W
$Ex_{u,p}$	exergy output rate considering pressure drop	W
$Ex_{d,p}$	exergy destruction due to pressure drop	W
F'	collector efficiency factor	
F_r	collector heat removal factor	
f	coefficient of friction	
h	enthalpy	J/kg
$h_{c,f\text{-}b}$	convective heat transfer coefficient between air and bottom plate	W/m^2 K
$h_{c,f\text{-}p}$	convective heat transfer coefficient between air and absorber plate	W/m^2 K
h_e	equivalent heat transfer coefficient	W/m^2 K
$h_{r,p\text{-}b}$	radiative heat transfer coefficient between absorber and bottom plate	W/m^2 K
h_w	wind heat transfer coefficient	W/m^2 K
H	solar air heater duct depth	m
I	radiation intensity	W/m^2
$I_{T,c}$	radiation incident on glass cover	W/m^2
IR	irreversibility	W
k_i	thermal conductivity of insulation	W/m K
k_a	thermal conductivity of air	W/m K
l	long way of mesh	m
L	spacing between covers	m
L_1	collector length	m
L_2	collector width	m
L_3	collector depth	m
m	mass flow rate	kg/s
M	number of glass cover	
p	pressure	N/m^2
P	roughness pitch	m
Pr	Prandtal's number	
Q	heat	W
q	heat per unit area	W/m^2
Re	Reynold's number	
s	short way of mesh, entropy	m J/kg K
S	absorbed flux	W/m^2
S_{gen}	entropy generation rate	W/K
T	temperature	K
T_{bm}	mean bottom plate temperature	K
T_{fm}	mean fluid temperature	K
T_{pm}	mean absorber plate temperature	K
U_b	bottom heat loss coefficient	W/m^2 K
U_l	over-all heat loss coefficient	W/m^2 K
U_s	side heat loss coefficient	W/m^2 K
U_t	top heat loss coefficient	W/m^2 K
V	velocity of air through collector duct	m/s
V_∞	wind velocity	m/s
W_P	pump-work	W

Greek symbols

β	tilt angle of collector surface	
δ_b	bottom insulation thickness	m
δ_s	side insulation thickness	m
Δp	pressure drop	N/m^2
η_{pm}	pump-motor efficiency	
μ	viscosity of air	N s/m^2
ρ	density of air	kg/m^3
τ	transmissivity	
$\tau\alpha$	transmissivity-absorptivity product	
σ	Stefan's constant	
ε_c	emissivity of cover	
ε_p	emissivity of absorber plate	

Subscripts

a	ambient
f	fluid (air)
$f\text{-}b$	fluid (air) to bottom plate
$f\text{-}p$	fluid (air) to absorber plate
G	glass
i	inlet
l	lost
o	outlet/exit
p	plate
r	rough
s	smooth
S	sun
T	tilted surface
u	useful

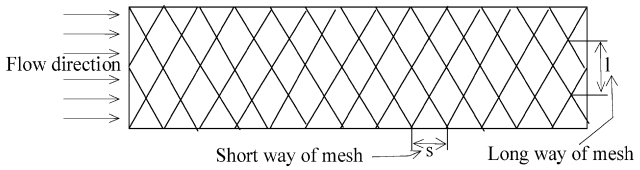

Fig. 1. Expanded metal mesh roughness geometry investigated by Ref. [5].

The commercially available wire mesh or expanded metal matrix is easy to fix on the absorber plate. Thus, the aim of present investigation is to carry out the performance evaluation of expanded metal mesh (Fig. 1) on the basis of energy augmentation ratio (*EAR*), effective energy augmentation ratio (*EEAR*) and exergy analysis based exergy augmentation ratio (*EXAR*). Based on *EXAR* the suitable design parameters of expanded metal mesh roughness geometry are also determined.

2. Thermodynamic modeling

2.1. Entropy generation during sun-solar air heater heat exchange process (a general analysis)

A thermodynamic frame work for minimum irreversibility during sun-solar air heater heat exchange process is constructed. The heat flux is received from the sun by an absorber and transferred to air flowing through the solar air heater. The solar heat flux falling on transparent cover of collector is less than extraterrestrial solar radiation. Thus, there is entropy generation during the process of radiation falling on collector glazing from outside the earth atmosphere, which is beyond our control except to keep the collector at optimum slope. The total insolation on transparent glass cover is partly delivered to flowing air as heat transfer and remaining is lost to ambient as heat loss. The entropy generation [7]

during this glass cover to air heat exchange process can be written using second law of thermodynamics as

$$\begin{aligned} S_{\text{gen},G\text{-air}} &= -I_{T,c}A_c/T_S + (I_{T,c}-S)A_c/T_a \\ &\quad + m(s_o - s_i) + Q_l/T_a \\ \Rightarrow S_{\text{gen},G\text{-air}} &= \left[SA_c/T_p - I_{T,c}A_c/T_S + (I_{T,c}-S)A_c/T_a\right] \\ &\quad + \left[m(s_o - s_i) + Q_l/T_a - SA_c/T_p\right] \end{aligned} \tag{1}$$

where $Q_l = SA_c - Q_u$ is heat loss from the air heater.

It is evident from first bracket term of above Eq. (1) that higher irreversibility takes place in absorption of radiation by absorber surface at a temperature quite less than the temperature of the sun as black body source. The second bracket term for a particular collector can be regarded as the entropy generation during heat transfer from absorber plate to flowing air.

Using $ds = \frac{c_p\,dT}{T} - \frac{dp}{\rho T}$ the entropy change of air in solar air heater duct can be written as

$$m(s_o - s_i) = mc_p \log\frac{T_o}{T_i} + mR\log\frac{p_1}{p_2} \cong mc_p \log\frac{T_o}{T_i} + \frac{m\Delta p}{\rho T_f}$$

where the first term represents the entropy change due to heat transfer and the second term is the entropy change caused by fluid friction. Thus higher friction losses will lead to more entropy change of air.

The exergy output rate delivered by a solar heater or exergy gain by air is given by

$$\begin{aligned} Ex_{u,p} &= m\left[(h_o - T_a s_o) - (h_i - T_a s_i)\right] \\ &= m\left[(h_o - h_i) - T_a(s_o - s_i)\right] \end{aligned} \tag{2}$$

$$\begin{aligned} \Rightarrow Ex_{u,p} &= Q_u - mT_a(s_o - s_i) \\ &= T_a\left[\frac{(SA_c - Q_l)}{T_a} - m(s_o - s_i)\right] \\ \Rightarrow Ex_{u,p} &= T_a\left[\frac{I_{T,c}A_c}{T_a} - \frac{I_{T,c}A_c}{T_S} \right. \\ &\quad - \left(-\frac{I_{T,c}A_c}{T_S} + \frac{(I_{T,c}-S)A_c}{T_a} \right. \\ &\quad \left.\left. + m(s_o - s_i) + \frac{Q_l}{T_a}\right)\right] \end{aligned}$$

$$Ex_{u,p} = T_a\left[I_{T,c}A_c\left(\frac{T_S - T_a}{T_S T_a}\right) - (S_{\text{gen},G\text{-air}})\right] \tag{3}$$

Thus, it can be said from Eq. (3) that maximization of exergy delivered by a solar heater is equivalent to minimization of entropy generation $S_{\text{gen},G\text{-air}}$ as defined above. Though the both $I_{T,c}A_c((T_S - T_a)/T_S T_a)$ and $(S_{\text{gen},G\text{-air}})$ are positive, but the exergy output of solar air heater for high flow Reynolds number may be negative due to higher pressure drop. Thus, the maximization of the exergy output instead of entropy generation minimization of solar air heater is more suitable quantity for the optimization.

2.2. Analysis of solar air heater

The collector under consideration consists of a flat glass cover and a flat absorber plate with a well insulated parallel bottom plate forming a passage of high duct aspect ratio through which the air to be heated flows as shown in Fig. 2. The heat gain by air may be calculated by following equations:

$$\begin{aligned} Q_u &= A_c\left[S - U_l(T_{pm} - T_a)\right] \\ &= A_c\left[\tau_g\alpha_p I_{T,c} - U_l(T_{pm} - T_a)\right] \end{aligned} \tag{4}$$

$$Q_u = mc_p(T_o - T_i) \tag{5}$$

$$Q_u = A_c F_r\left[S - U_l(T_i - T_a)\right] \tag{6}$$

The collector heat removal factor F_r is given by

$$F_r = \frac{mc_p}{U_l A_c}\left[1 - e^{(-U_l A_c F'/mc_p)}\right] \tag{7}$$

The collector efficiency factor F' is

$$F' = \left(1 + \frac{U_l}{h_e}\right)^{-1} \tag{8}$$

where the equivalent heat transfer coefficient h_e is calculated by

$$h_e = h_{c,f\text{-}p} + \frac{h_{r,p\text{-}b}h_{c,f\text{-}b}}{(h_{r,p\text{-}b} + h_{c,f\text{-}b})} \tag{9}$$

The $h_{c,f\text{-}p}$ and $h_{c,f\text{-}b}$ are heat transfer coefficients due to convection, respectively, from absorber plate to flowing air, and from bottom plate to flowing air. The $h_{r,p\text{-}b}$, is heat transfer coefficient due to radiation from absorber plate to bottom plate.

The mean absorber plate temperature is obtained from Eqs. (4) and (6), and is given by

$$T_{pm} = T_a + \frac{Q_l}{U_l A_c} = T_i + \frac{Q_u}{A_c F_r U_l}(1 - F_r) \tag{10}$$

The mean fluid temperature is given by

$$T_{fm} = T_i + \frac{Q_u}{A_c F_r U_l}\left(1 - \frac{F_r}{F'}\right) \tag{11}$$

Considering solar air heater [Fig. 2] as a control volume (CV), the exergy balance [6] for this CV can be written as

$$Ex_i + Ex_{c,S} + Ex_W = Ex_o + IR \tag{12}$$

where Ex_i and Ex_o are the exergy associated with mass flow of collector fluid entering and leaving the CV; $Ex_{c,S}$ is exergy of solar radiation falling on glass cover; Ex_W is exergy of work input required to pump the fluid through FPSC, and IR is irreversibility or exergy loss of the process. The exergy balance (Eq. (12)) can be written as

$$IR = Ex_{c,S} - (Ex_o - Ex_i - Ex_W) \tag{13}$$

The bracket term of Eq. (13) represents the useful exergy or exergy output rate delivered by the solar collector. The exergy of solar radiation $Ex_{c,S}$ falling on glass cover is fixed for a particular instant, thus minimization of irreversibility is equivalent to maximization of exergy output rate delivery of collector. The useful exergy or exergy output rate 'Ex_u' delivered by a solar collector using exergy balance equation for collector fluid ignoring pressure drop/pumping work W_p or Ex_W is given by

$$\begin{aligned} Ex_u &= m\left[(h_o - T_a s_o) - (h_i - T_a s_i)\right] \\ &= m\left[(h_o - h_i) - T_a(s_o - s_i)\right] \end{aligned} \tag{14}$$

For an incompressible fluid or perfect gas it can be written as

$$\begin{aligned} Ex_u &= mc_p\left[(T_o - T_i) - T_a\ln(T_o/T_i)\right] \\ &= Q_u - mc_p T_a \ln(T_o/T_i) \end{aligned} \tag{15}$$

The actual exergy output rate $Ex_{u,p}$ delivered considering pressure drop of collector fluid is

$$Ex_{u,p} = Ex_u - Ex_{d,p} \tag{16}$$

where the exergy destruction $Ex_{d,p}$ due to pressure drop is

$$Ex_{d,p} = \frac{T_a}{T_i}W_p \tag{17}$$

The pump work W_p is calculated by

$$W_p = m\Delta p/(\eta_{pm}\rho) \tag{18}$$

where the pump-motor efficiency η_{pm} is taken equal to 0.85.

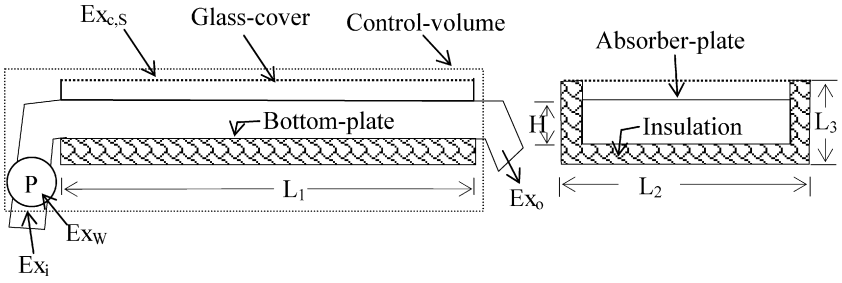

Fig. 2. Flat plate solar air heater.

2.3. Heat-transfer and pressure drop

The overall heat loss coefficient U_l is sum of U_b, U_s and U_t and is given by

$$U_l = U_b + U_s + U_t \tag{19}$$

where $U_b = k_i/\delta_b$ and $U_s = (L_1 + L_2)L_3k_i/L_1L_2\delta_s$.

Thus, U_b and U_s for a particular collector can be regarded as constant while U_t varies with temperature of absorber plate, number of glass covers and other parameters. The top heat loss coefficient U_t is evaluated empirically [14] by

$$U_t = \left[\frac{M}{\left(\frac{C}{T_{pm}}\right)\left(\frac{T_{pm}-T_a}{M+f'}\right)^{0.252}} + \frac{1}{h_w}\right]^{-1} + \left[\frac{\sigma(T_{pm}^2 + T_a^2)(T_{pm} + T_a)}{\frac{1}{\varepsilon_p + 0.0425M(1-\varepsilon_p)} + \frac{2M+f'-1}{\varepsilon_c} - M}\right] \tag{20}$$

In which

$$f' = \left(\frac{9}{h_w} - \frac{9}{h_w^2}\right)\left(\frac{T_a}{316.9}\right)(1 + 0.091M),$$

$$C = 204.429\left(\frac{(\cos\beta)^{0.252}}{L^{0.24}}\right)$$

and h_w is the heat-transfer coefficient due to convection at the top of cover due to wind. The h_w is calculated by the following relation suggested by McAdams as given in Duffie and Beckman [15]

$$h_{c,c\text{-}a} = h_w = 5.7 + 3.8V_\infty \tag{21}$$

The radiation heat transfer coefficient $h_{r,p\text{-}b}$ between absorber plate and bottom plate is given by

$$h_{r,p\text{-}b}(T_{pm} - T_{bm}) = \frac{\sigma(T_{pm}^4 - T_{bm}^4)}{\left(\frac{1}{\varepsilon_p} + \frac{1}{\varepsilon_b} - 1\right)} \tag{22}$$

For small temperature difference between T_{pm} and T_{bm} on absolute scale the above Eq. (22) can be written as

$$h_{r,p\text{-}b} \cong \frac{4\sigma T_{av}^3}{\left(\frac{1}{\varepsilon_p} + \frac{1}{\varepsilon_b} - 1\right)}$$

where $T_{av} = (T_{pm} + T_{bm})/2$ and T_{av} is taken equal to T_{fm} in iterative calculation using the same logic.

For smooth duct the convection heat transfer coefficients between flowing air and absorber plate $h_{c,f\text{-}p}$ and flowing air and bottom plate $h_{c,f\text{-}b}$ are assumed equal. The following correlation for air, for fully developed turbulent flow (if length to equivalent diameter ratio exceeds 30) with one side heated and the other side insulated [16] is appropriate:

$$Nu = \frac{h_{c,f\text{-}p}d_e}{k_a} = 0.0158(Re)^{0.8} \tag{23a}$$

If the flow is laminar then following correlation by Mercer from Duffie and Beckman [15] for the case of parallel smooth plates with constant temperature on one plate and other plate insulated is appropriate:

$$Nu = \frac{h_{c,f\text{-}p}d_e}{k_a} = 4.9 + \frac{0.0606\left(Re\,Pr.\frac{d_e}{L_1}\right)^{0.5}}{1 + 0.0909\left(Re\,Pr.\frac{d_e}{L_1}\right)^{0.7}(Pr)^{0.17}} \tag{23b}$$

For artificially roughened solar air heater by expanded metal mesh at the back side of absorber plate, the equivalent heat transfer coefficient (for Re greater than 1900) is calculated as [5]

$$Nu = \frac{h_e d_e}{k_a} = 4.0 \times 10^{-4}(Re)^{1.22}\left(\frac{e}{d_e}\right)^{0.625}\left(\frac{s}{10e}\right)^{2.22} \times \left(\frac{l}{10e}\right)^{2.66} \times \exp\left[-1.25\left(\ln\frac{s}{10e}\right)^2\right] \times \exp\left[-0.824\left(\ln\frac{l}{10e}\right)^2\right] \tag{23c}$$

The characteristic dimension or equivalent diameter of duct is given by

$$d_e = \frac{2L_2H}{(L_2 + H)} \tag{24}$$

For a particular Reynolds number Re, the velocity of flow is calculated by

$$V = \frac{\mu\,Re}{\rho d_e} \tag{25}$$

While the mass flow rate is calculated by

$$m = L_2HV\rho = \frac{\mu(L_2 + H)Re}{2} \tag{26}$$

The pressure loss Δp through air heater duct is calculated by

$$\Delta p = \frac{4fL_1V^2\rho}{2d_e} \tag{27}$$

If $Re = \rho V d_e/\mu \leqslant 2300$, i.e. laminar flow then coefficient of friction for smooth duct is calculated by

$$f = \frac{16}{Re} \tag{28a}$$

otherwise the coefficient of friction f for the turbulent flow in smooth air duct is calculated from Blasius equation, which is

$$f = 0.0791(Re)^{-0.25} \tag{28b}$$

For artificially roughened solar air heater by expanded metal mesh at the back side of absorber plate, the coefficient of friction f (for Re greater than 1900) is calculated as [5]

$$f = 0.815(Re)^{-0.361}\left(\frac{10e}{d_e}\right)^{0.591}\left(\frac{l}{e}\right)^{0.266}\left(\frac{s}{10e}\right)^{-0.19} \tag{28c}$$

As at lower Re the variation in Nu with roughness parameters is insignificant, hence, for Re less than 1900, the heat transfer and coefficient of friction correlation for smooth duct are used.

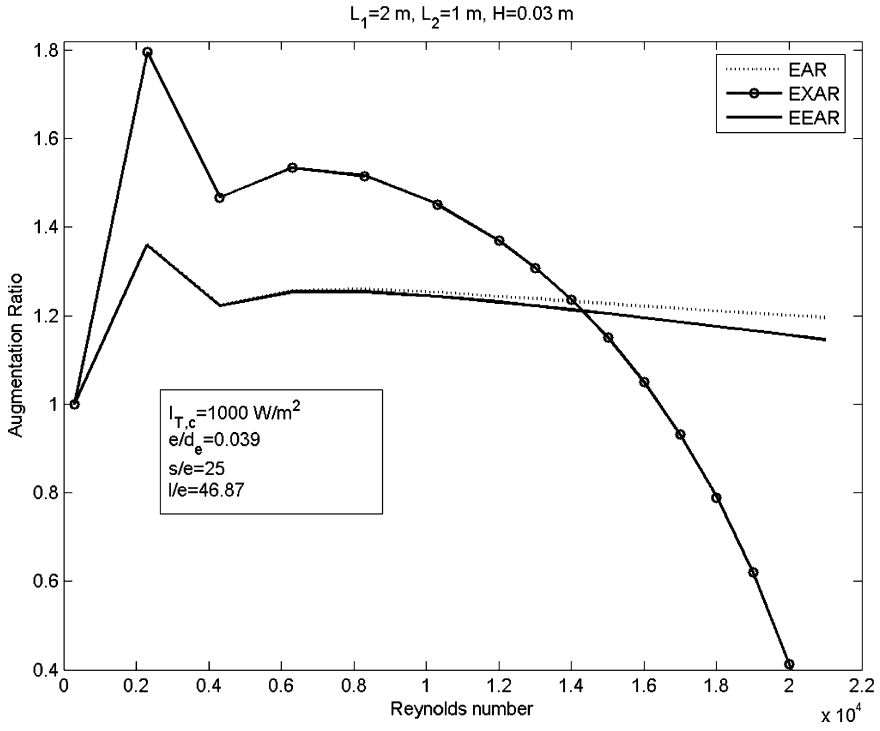

Fig. 3. Augmentation ratios vs. Reynolds number for $H = 0.03$ m.

2.4. Performance parameters: EAR, EEAR and EXAR

The artificial roughness geometry in the absorber plate of solar air heater can be regarded as design changes whose ultimate purpose is to improve the thermodynamic performance. The effect of artificial roughness geometry on thermodynamic performance can be evaluated by comparing the performance of solar air heater duct before and after the implementation of the artificial roughness geometry. Thus the augmentation ratio term has been defined as ratio of performance of roughened duct to smooth duct.

The energy augmentation ratio (*EAR*) is ratio of heat gain by air in a roughened duct to smooth duct, and is calculated by

$$EAR = \frac{Q_{u,r}}{Q_{u,s}} \tag{29}$$

The effective energy augmentation ratio (*EEAR*) is ratio of net thermal energy gain by air in a roughened duct to smooth duct. The net thermal energy gain [17] takes in account the pump work and it is obtained by subtracting the equivalent thermal energy to produce the pump work from useful heat gain by air heater. *EEAR* is calculated by

$$EEAR = \left(Q_{u,r} - \frac{W_{p,r}}{C_f}\right) \Big/ \left(Q_{u,s} - \frac{W_{p,s}}{C_f}\right) \tag{30}$$

The conversion factor C_f takes in account various efficiencies (thermal to mechanical), and is taken 0.2.

The enhancement in heat transfer, by using artificial roughness geometry, is also accompanied with substantial increase in pumping power to blow the air. Thus the maximum exergy delivery based on second law of thermodynamics is a solid thermodynamic basis for evaluating the merit of artificial roughness geometry. The exergy augmentation ratio (*EXAR*) is calculated by

$$EXAR = (Ex_{u,p})_r / (Ex_{u,p})_s \tag{31}$$

In this paper, the above mentioned performance parameters have been used as basis for the performance evaluation.

3. Numerical calculations

For a collector configuration, system properties and operating conditions numerical calculations have been carried out to evaluate the *EAR*, *EEAR* and *EXAR*. The thermal behavior of artificially roughened solar air heater is similar to that of usual flat plate conventional air heater; therefore, the usual procedures of calculating the absorbed irradiation and the heat losses are used. First a set of system roughness parameter namely $\frac{e}{d_e}$, $\frac{l}{e}$ and $\frac{s}{e}$ is selected for the analysis. The heat gain, net thermal energy gain and exergy output rate are determined separately for smooth as well as roughened duct in order to evaluate the augmentation ratios. For a particular given value of *Re* first initial values of T_{pm} and T_{fm} are assumed according to inlet temperature of air and various heat transfer coefficients are calculated. The new values of T_{pm} and T_{fm} are calculated using Eqs. (19)–(26) and (6)–(11). If the calculated new values of T_{pm} and T_{fm} are different than the previously assumed values then the iteration is repeated with these new values till the absolute differences of new value and previous value of, mean plate as well as mean fluid temperature, are less than or equal to 0.05. Air properties are determined at T_{fm} by interpolation from air properties [18]. The heat gain and outlet temperature of air are calculated from Eqs. (5) and (6). The exergy output rate is calculated using Eqs. (27)–(28) and (15)–(18). The same procedure is adopted for smooth as well as rough duct. The various augmentation ratios are evaluated from Eqs. (29)–(31). In order to obtain the results numerically, codes are developed in Matlab-7 using the following parameters: $L_1 = 2$ m, $L_2 = 1$ m, $A_c = 2$ m^2, $H = 3.0$ cm, $K_i = 0.04$ W/m K, $L = 4$ cm, $\delta_b = 6$ cm, $\delta_s = 4$ cm, $\varepsilon_p = 0.95$, $\varepsilon_c = 0.88$, $\varepsilon_b = 0.95$, $\alpha_p = 0.95$, $\tau_g = 0.88$, $\tau\alpha = 0.9$, $\beta = 30°$, $T_{fi} = 30\,°$C, $T_a = 30\,°$C, $V_\infty = 1.5$ m/s, $T_S = 5600$ K and $I_{T,c} = 1000$ W/m^2.

The performance evaluation has also been carried out for various values of duct depth (H) and $I_{T,c}$.

4. Results and discussion

Figs. 3–4 show the variations of *EAR*, *EEAR* and *EXAR* with Reynolds number to point out the differences in these augmen-

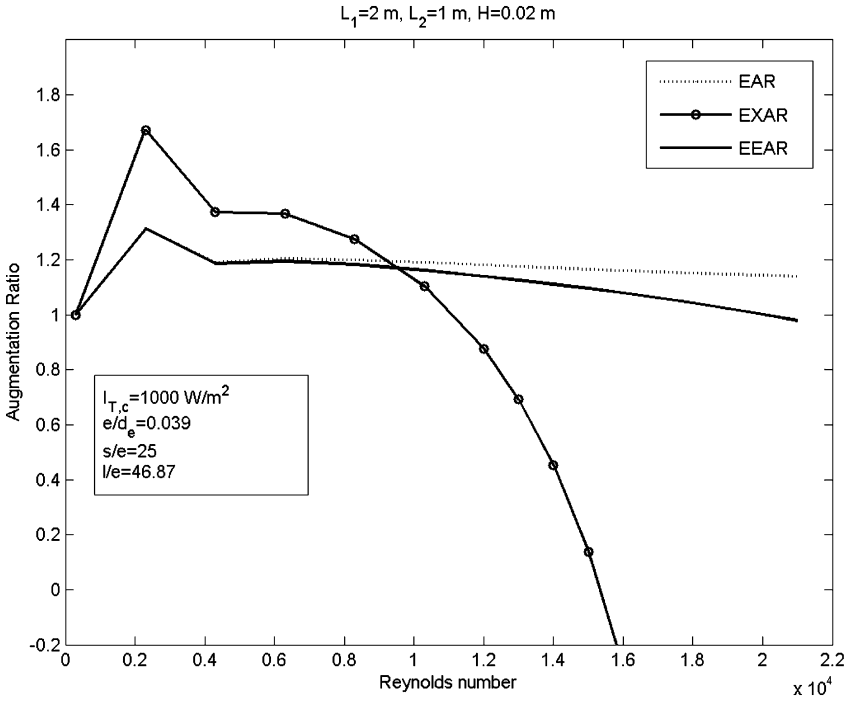

Fig. 4. Augmentation ratios vs. Reynolds number for $H = 0.02$ m.

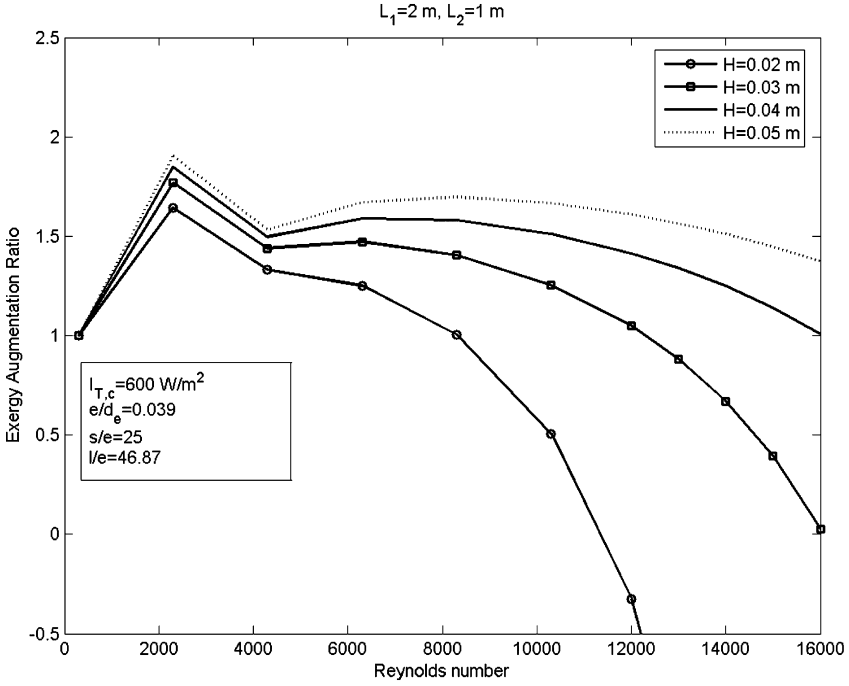

Fig. 5. Exergy augmentation ratio vs. Reynolds number for various duct depth.

tation ratios. It is evident from Figs. 3–4 that the augmentation ratios decrease with *Re*. This is due to the fact that the artificial roughness creates the turbulence by breaking the laminar/viscous sub-layer existing in a turbulent boundary layer. The thickness of laminar sub-layer reduces with increase in *Re*, hence, the augmentation ratios decrease with *Re*. It may also be observed that augmentation ratios are higher for larger duct depth, thus the roughness geometry is more effective at low *Re* and larger duct depth. It can also be seen that *EAR* and *EEAR* decreases little with *Re* and up to some *Re* the *EEAR* is close to *EAR* as small pump work is required in comparison to quantity of heat energy collected. The quality (exergy) of heat energy collected by a solar air heater is very small in comparison to quantity of heat energy collected. For higher *Re* the quantity of heat energy collected varies little while the pump work increases with power law. The useful exergy output, which is difference of quality of heat energy collected and required pump work, reduces with *Re*. Thus the rate of decrease of *EXAR* with *Re* is higher than rate of decrease of *EEAR* and *EAR*.

It may happen for higher *Re* that the required pump work exceeds the exergy of heat energy collected and useful exergy output becomes negative. The *EEAR* and *EAR* based criteria signifies that the roughened duct is better up to very high value

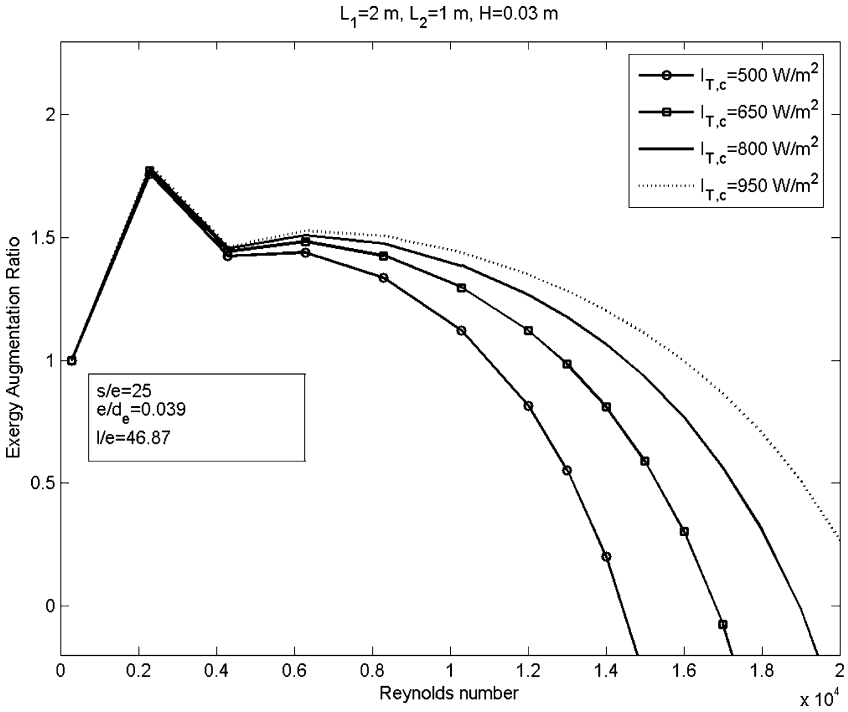

Fig. 6. Exergy augmentation ratio vs. Reynolds number for various intensity of solar radiation.

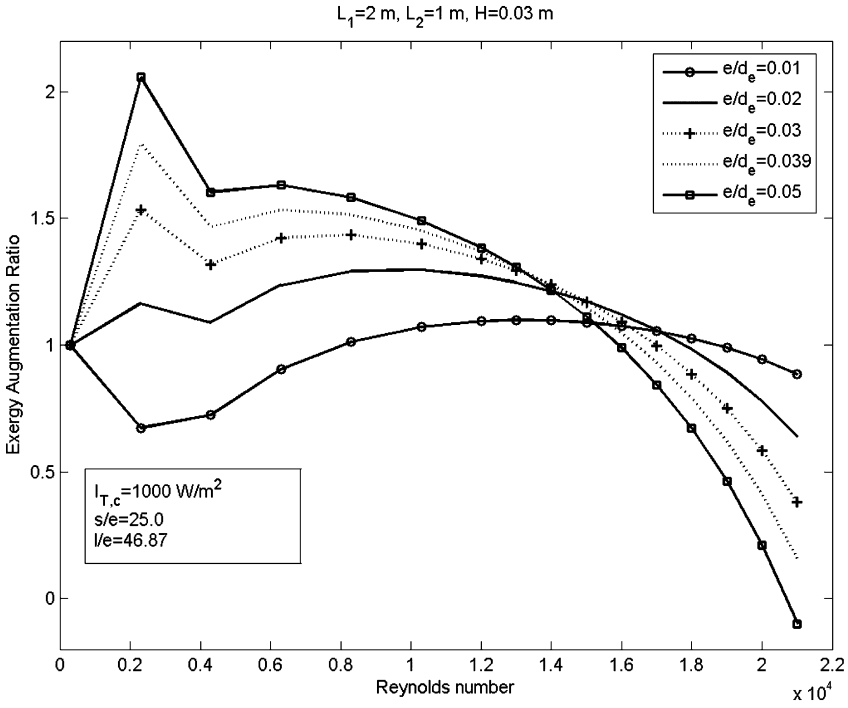

Fig. 7. Exergy augmentation ratio vs. Reynolds number for various relative roughness heights.

of *Re*; while the *EXAR* becomes less than unity beyond some value of *Re* depending on the duct parameters, e.g., duct depth (as the pump work is strong function of duct depth). Thus, the *EXAR* is more meaningful criterion for performance evaluation. Further, the *EAR* based criterion does not give the optimum parameters of roughness geometry, and recommends to use higher e/d_e and lower s/e and l/e in order to create more turbulence.

It may be observed (Figs. 3–4) that the rate of decrease of *EXAR* is higher for the solar air heater having lower duct depth. The range of *Re* up to which *EXAR* is more than unity reduces with decrease in duct depth. Fig. 5 also shows that *EXAR* increases with increase in duct depth; as the irreversibility due to pressure drop or pump work is small for higher value of duct depth. Fig. 6 shows the variation of *EXAR* with *Re* for various values of solar radiation falling on transparent glass cover $I_{T,c}$. It is evident that *EXAR* decreases with decrease in $I_{T,c}$. The range of *Re* up to which roughened duct is better reduces with decrease in $I_{T,c}$. The range of *Re* must be low and flow rate should be controlled as per radiation intensity $I_{T,c}$ variation throughout the day.

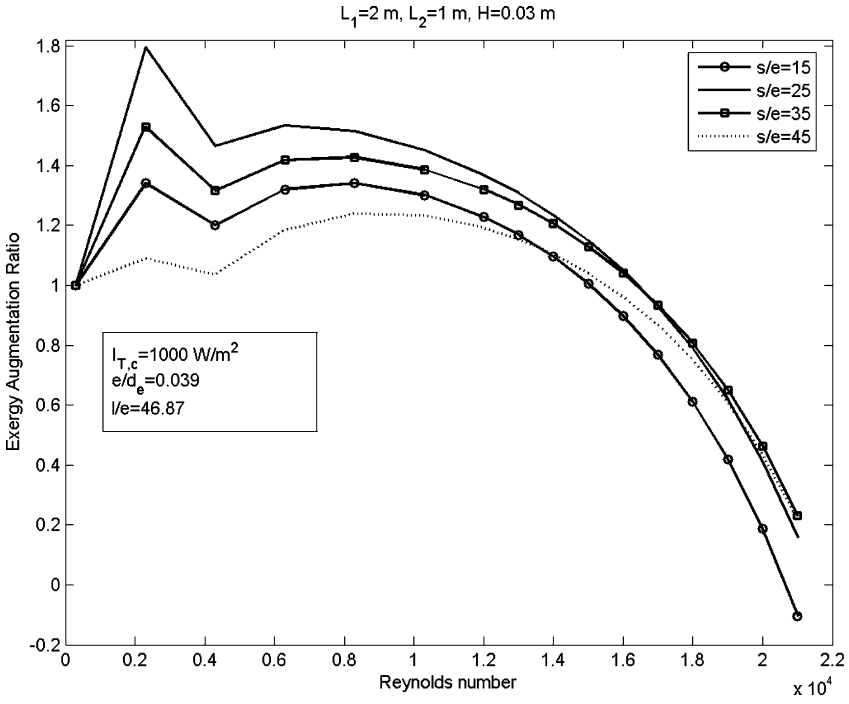

Fig. 8. Exergy augmentation ratio vs. Reynolds number for various relative short way lengths.

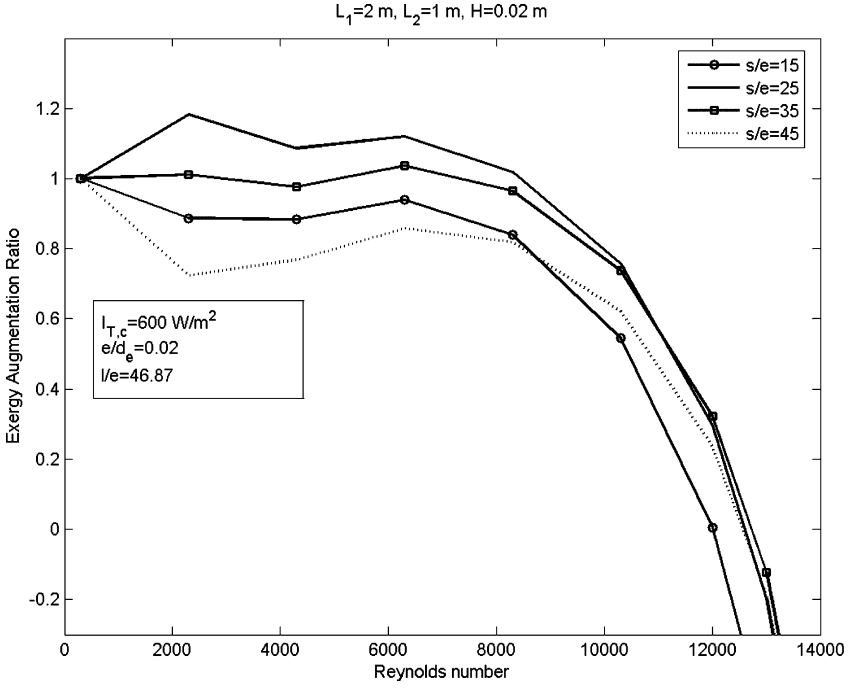

Fig. 9. Exergy augmentation ratio vs. Reynolds number for various relative short way lengths.

The variation of *EXAR* with *Re* for various values of e/d_e, and fixed value of other parameters is shown in Fig. 7. It is clear from Fig. 7 that *EXAR* increases with e/d_e for low range of *Re* but for higher range of *Re*, the trend is reversed mainly due to large pump work requirement. The variation of *EXAR* with *Re* for various values of s/e, and fixed value of other parameters is shown in Fig. 8. It can be seen that as s/e increases the *EXAR* first increases and then decreases. It is evident from Fig. 9 that same pattern is observed for other values of $I_{T,c}$, e/d_e and H but for the same value of l/e (46.87). It can be seen (Figs. 8–9) that the maximum *EXAR* is attained for s/e equal to 25 for the given value of l/e. Thus, it can be shown that the best exergetic performance is achieved for an angle of attack of about 60° as $\tan^{-1}(46.87/25) = 61.9°$. It has also been observed by Saini and Saini [5] that for a fixed value of s/e equal to 25, the average Nusselt number increases with an increase in l/e from 25 to 46.87, but for l/e larger than 46.87, the Nusselt number decreases. Thus an angle of attack of about 60 °C also corresponds to the maximum heat transfer coefficient. Fig. 10 shows the variation of *EXAR* with *Re* for various values of l/e and fixed value of other parameters. It can be seen that for the given value of s/e (25) the higher *EXAR* is achieved for the values of l/e in between 40–55. Thus, it can be again emphasized that the

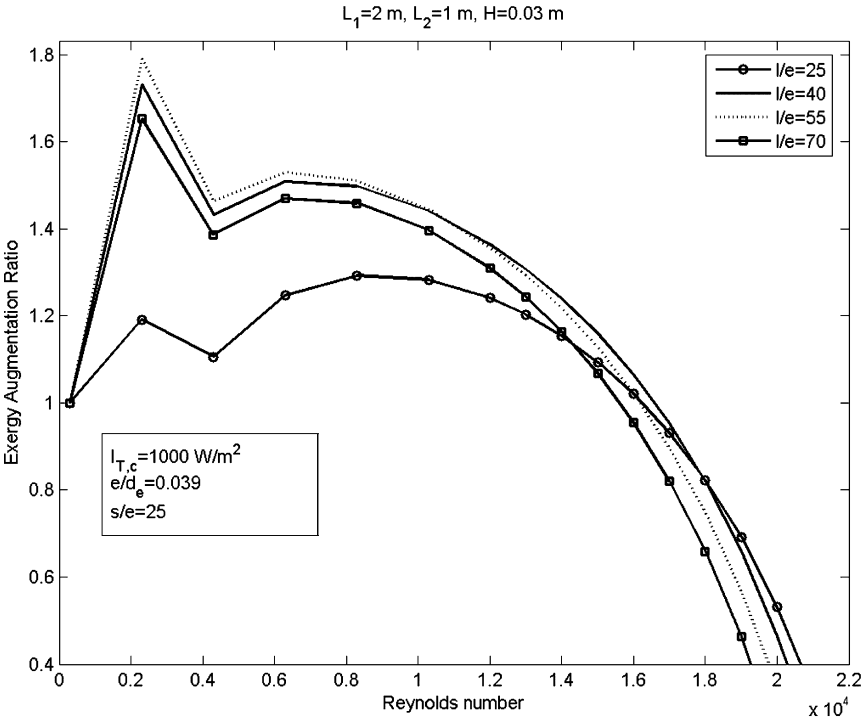

Fig. 10. Exergy augmentation ratio vs. Reynolds number for various long way lengths.

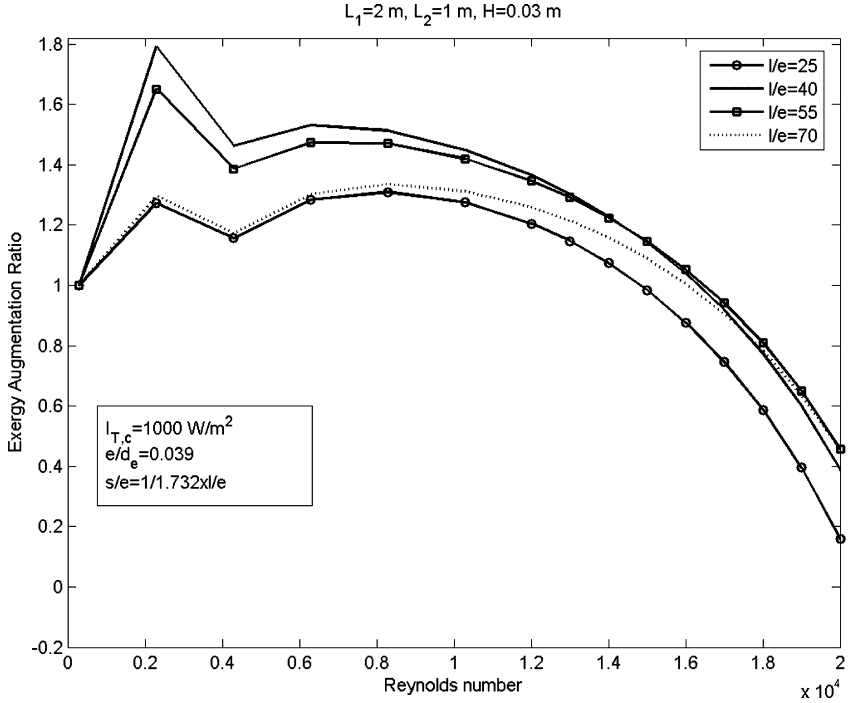

Fig. 11. Exergy augmentation ratio vs. Reynolds number for various long way length and corresponding short way length at an angle of attack of 60°.

angle of attack must be around 60°. Fig. 11 shows the variation of *EXAR* with *Re* for various values of l/e, s/e corresponding to angle of attack of 60° and fixed value of other parameters. It is evident that $l/e = 40$ gives highest *EXAR* followed by $l/e = 55$; thus for the better exergetic performance the l/e may be 40–55.

5. Conclusion

The augmentation ratios are improved by using expanded metal mesh type roughened geometries in the duct of solar air heater. The *EAR* and *EEAR* based criteria suggest the use of the roughened geometries up to very large value of *Re*. The *EXAR* based criteria shows that the *EXAR* decreases with *Re*, and becomes less than unity and may be even negative when exergy of pump work required exceeds the exergy of heat energy collected by roughened solar air heater. Thus *EXAR* provides the meaningful criteria for performance evaluation. The *EXAR* is more than unity for larger flow cross section area of solar air heater duct along with low *Re* range and higher intensity of solar radiation. The *EXAR* increases with roughness height for low range of *Re*. The long way length

l/e of expanded metal mesh may be desirable in the range 40–55 with an angle of attack of 60° for higher *EXAR*.

Acknowledgement

The author (M.K. Gupta) gratefully acknowledges Ujjain Engineering College, Ujjain, M.P. (India) and IIT Delhi (India), for sponsorship under quality improvement program of government of India.

References

[1] Varun, R.P. Saini, S.K. Singal, A review on roughness geometry used in solar air heaters, Solar Energy 81 (2007) 1340–1350.
[2] R.L. Webb, E.R.G. Eckert, R.J. Goldstein, Heat transfer and friction in tubes with repeated-rib roughness, Int. J. Heat Mass Transfer 14 (1971) 601–617.
[3] J.C. Han, L.R. Glicksman, W.M. Rohsenow, An investigation of heat transfer and friction for rib-roughened surfaces, Int. J. Heat Mass Transfer 21 (1978) 1143–1156.
[4] M.K. Mittal, Varun, R.P. Saini, S.K. Singal, Effective efficiency of solar air heaters having different types of roughness elements on the absorber plate, Energy 32 (2007) 739–745.
[5] R.P. Saini, J.S. Saini, Heat transfer and friction factor correlations for artificially roughened ducts with expanded metal mesh as roughened element, Int. J. Heat Mass Transfer 40 (1997) 973–986.
[6] T.J. Kotas, The Exergy Method of Thermal Plant Analysis, Butterworths, London, 1985.
[7] A. Bejan, Entropy Generation through Heat and Fluid Flow, Wiley-Interscience, New York, 1982.
[8] H.H. Ozturk, Y. Demirel, Exergy-based performance analysis of packed-bed solar air heaters, Int. J. Energy Res. 28 (2004) 423–432.
[9] M.A. Rosen, I. Dincer, A study of industrial steam process heating through exergy analysis, Int. J. Energy Res. 28 (2004) 917–930.
[10] M.K. Gupta, S.C. Kaushik, Exergetic performance evaluation and parametric studies of solar air heater, Energy (2008), doi:10.1016/j.energy.2008.05.010.
[11] A. Ucar, M. Inalli, Thermal and exergy analysis of solar air collectors with passive augmentation techniques, Int. Com. in Heat and Mass Transfer 33 (2006) 1281–1290.
[12] H. Esen, Experimental energy and exergy analysis of a double-flow solar air heater having different obstacles on absorber plates, Building and Environment 43 (2008) 1046–1054.
[13] A. Layek, J.S. Saini, S.C. Solanki, Second law optimization of a solar air heater having chamfered rib–groove roughness on absorber plate, Renewable Energy 32 (2007) 1967–1980.
[14] A. Malhotra, H.P. Garg, A. Palit, Heat loss calculation of flat plat solar collectors, J. Thermal Energy 2 (1981) 2.
[15] J.A. Duffie, W.A. Beckman, Solar Engineering of Thermal Processes, Wiley, New York, 1991.
[16] W.M. Kays, Convective Heat and Mass Transfer, McGraw-Hill, New York, 1966.
[17] A. Cortes, R. Piacentini, Improvement of the efficiency of a bare solar collector by means of turbulent promoters, Appl. Energy 36 (1990) 253–261.
[18] S.P. Sukhatme, Solar Energy: Principles of Thermal Collection and Storage, Tata McGraw-Hill, New Delhi, India, 1987.